

Letters

Submodule Fault-Tolerant Control of Modular Multilevel Matrix Converters With Adaptive Optimum Common-Mode Voltage Injection

Chao Wang , Student Member, IEEE, Zedong Zheng , Senior Member, IEEE, Kui Wang , Senior Member, IEEE, and Yongdong Li, Senior Member, IEEE

Abstract—The modular multilevel matrix converter (M3C) is an attractive topology for high-voltage and high-power direct ac-to-ac power conversion applications. SM fault-tolerant control is of great importance for the M3C. This letter proposes an optimum common-mode voltage injection (CMV) method which can maximize the input and output voltage ranges of the M3C after nonredundant submodules (SMs) are failed. The injected optimum CMV is calculated in real-time according to the relationship between the fundamental reference voltage and maximum available voltage of each branch, which can be adaptive to different load and fault conditions. The operating area of the M3C after the fault when employing this method is also discussed. Experimental results implemented on an M3C prototype with three SMs in each branch are presented to validate the proposed method and analysis.

Index Terms—Adaptive optimum common-mode voltage (CMV), fault-tolerant control, modular multilevel matrix converter (M3C), submodule (SM) fault.

I. INTRODUCTION

THE MODULAR multilevel matrix converter (M3C) is capable of realizing direct ac-to-ac power conversion, which has gained much attention in several applications, such as variable-speed motor drive [1], low-frequency power transmission [2], offshore wind energy conversion [3], [4], and pumped hydro storage plants [5].

The circuit topology of the M3C is presented in Fig. 1, which directly connects two three-phase systems by nine branches. Each branch consists of N cascaded full-bridge submodules (SMs) and a branch inductor L_b . Similar to the traditional dc-ac modular multilevel converter (MMC), when nonredundant SMs in the M3C are failed, the maximum available branch voltages may not be able to support the input-output voltage difference, which affects the stable operation of the M3C. Therefore, to further enhance the reliability of the M3C in these applications,

Manuscript received December 6, 2021; revised January 12, 2022; accepted January 18, 2022. Date of publication January 27, 2022; date of current version March 24, 2022. This work was supported by the National Natural Science Foundation of China under Grant 51777110. (Corresponding author: Kui Wang.)

The authors are with the Department of Electrical Engineering, State Key Laboratory of Power System, Tsinghua University, Beijing 100084, China (e-mail: wangchao16@mails.tsinghua.edu.cn; zzd@tsinghua.edu.cn; wangkui@tsinghua.edu.cn; liyid@mail.tsinghua.edu.cn).

Color versions of one or more figures in this article are available at <https://doi.org/10.1109/TPEL.2022.3146249>.

Digital Object Identifier 10.1109/TPEL.2022.3146249

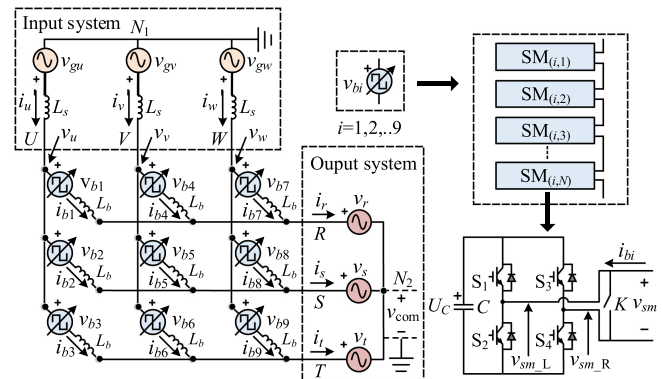


Fig. 1. Circuit configuration of the M3C.

special measures should be taken to realize the fault ride-through of nonredundant SMs.

This kind of problem has been widely studied in the MMC. The basic idea is to avoid overmodulation by injecting common-mode voltage (CMV) in output phase voltages. However, the key point is what kind of CMV can maximize the output voltage range after the fault within the limited available range of the CMV, which can be treated as the optimum CMV. A method based on the neutral shift (NS) of ac-side voltages is first proposed in [6]. However, it is not necessarily optimum when only the NS of the ac-side is employed. To take advantage of more degrees of freedom, a strategy that combines the NS of the ac and dc side is proposed in [7]. Based on the method proposed in [7], the optimum NS combinations which can maximize the output voltage range when there are different numbers of faulty SMs in each branch are presented in [8], which are obtained by numerical calculation and need to be stored as a lookup table for utilization. In addition, two methods are proposed in [9] and [10] to solve the fault-tolerant problem of the back-to-back MMC. In [9], a method that increases the capacitor voltages of healthy SMs based on the NS method is proposed. By gradually increasing the capacitor voltages of the healthy SMs after the fault, the output voltage of the MMC can gradually return to its rated value. Another method that increases the output voltage of the inverter-side MMC after the fault by reducing the dc-link voltage is proposed in [10]. This method can increase the output voltage amplitude compared with the optimum NS combination

proposed in [8], and it does not require a neutral-voltage shift which produces CMV. However, since the modulation index of the rectifier-side MMC is generally fixed and close to 1, the reduction of the dc-link voltage is limited, which limits the feasible region of this method.

Similar to the NS method employed in the MMC, a method that simultaneously shifts the input and output ac voltage is proposed in [11] to realize the fault-tolerant control of the M3C. The overmodulation of each branch is avoided by adjusting the neutral-point voltages of the input and output sides. However, the voltage waveforms of nine branches of the M3C change along with the load frequency and initial load phase angle (ILPA). Therefore, the optimized NS voltages which can enlarge the input and output voltage range (IOVR) as much as possible are related not only to the numbers of failed SMs in each branch but also to the load frequency and ILPA. Even though the numerical method is utilized to calculate the optimum results, the results are quite complex and difficult to be stored as a lookup table since they are related to multidimensional variables. Moreover, the injected CMV by the NS method is a combination of input and output fundamental voltages, which is just a specific form and not all frequency components are considered. Therefore, it may not necessarily maximize the IOVR.

This letter proposes a simple but effective method to determine the optimum CMV for the M3C after nonredundant SMs are failed. The basic principle is that when the fundamental reference voltage of a certain branch exceeds the limitation of its available voltage, the value of the excess part is taken as the CMV to be injected in each branch. Consequently, the reference voltage of this branch is limited to its maximum or minimum available value. Meanwhile, as long as the calculated CMV is within the available range of the CMV, it is a feasible solution that can also avoid the overmodulation of other branches. Since the proposed method always uses the CMV with the minimum amplitude to avoid overmodulation of each branch at any moment, the injected CMV can automatically maximize the IOVR, which is the optimum solution. Moreover, considering that the injected CMV is calculated in real-time according to the fundamental branch voltages, it can be adaptive to various conditions without the requirement of complex offline calculation and the storage of lookup tables, which is more convenient to be utilized than the existing NS method.

II. BASIC OPERATING PRINCIPLES OF THE M3C

Ignoring the voltage drop on the grid-connect inductor L_s , the phase voltages of the input and output sides, i.e., v_x ($x = u, v, w$) and v_y ($y = r, s, t$), can be defined as (1), where θ is the ILPA. In (1), $\omega_1 = 2\pi f_1$ and $\omega_2 = 2\pi f_2$, where f_1 and f_2 are the input and output frequencies, respectively.

$$\begin{aligned} v_x &\approx v_{gx} = \hat{v}_{g1} \cos(\omega_1 t + \alpha_x), \alpha_u \\ &= 0, \alpha_v = -2\pi/3, \alpha_w = 2\pi/3 \\ v_y &= \hat{v}_{m2} \cos(\omega_2 t + \alpha_y + \theta), \alpha_r \\ &= 0, \alpha_s = -2\pi/3, \alpha_t = 2\pi/3 \end{aligned} \quad (1)$$

According to Kirchoff's voltage law, the basic mathematical model of the M3C can be derived as (2), where v_{com} denotes the CMV between the neutral points N_1 and N_2 .

$$\begin{aligned} &\begin{bmatrix} v_u - v_r & v_v - v_r & v_w - v_r \\ v_u - v_s & v_v - v_s & v_w - v_s \\ v_u - v_t & v_v - v_t & v_w - v_t \end{bmatrix} - v_{com} \begin{bmatrix} 1 & 1 & 1 \\ 1 & 1 & 1 \\ 1 & 1 & 1 \end{bmatrix} \\ &= L_b \frac{d}{dt} \begin{bmatrix} \dot{i}_{b1} & \dot{i}_{b4} & \dot{i}_{b7} \\ \dot{i}_{b2} & \dot{i}_{b5} & \dot{i}_{b8} \\ \dot{i}_{b3} & \dot{i}_{b6} & \dot{i}_{b9} \end{bmatrix} + \begin{bmatrix} v_{b1} & v_{b4} & v_{b7} \\ v_{b2} & v_{b5} & v_{b8} \\ v_{b3} & v_{b6} & v_{b9} \end{bmatrix} \end{aligned} \quad (2)$$

Neglecting the voltage drop on L_b , the fundamental branch voltages without v_{com} injection, i.e., $v_{bi,0}$ ($i = 1, 2, \dots, 9$), are nearly equal to the differences of the corresponding input and output phase voltages. For instance, $v_{b1,0}$ can be expressed as follows:

$$v_{b1,0} \approx v_u - v_r. \quad (3)$$

Considering that the possible maximum value of $v_{bi,0}$ equals $\hat{v}_{g1} + \hat{v}_{m2}$, the modulation index of the M3C, i.e., m , can be defined as (4), which represents the IOVR. The optimum CMV after nonredundant SM faults should maximize the maximum available value of m , i.e., m_{max} .

$$m = (\hat{v}_{g1} + \hat{v}_{m2})/NU_C. \quad (4)$$

The branch voltage after v_{com} injection, $v_{bi,com}$, is derived as follows:

$$v_{bi,com} = v_{bi,0} - v_{com}. \quad (5)$$

III. PROPOSED ADAPTIVE OPTIMUM COMMON-MODE VOLTAGE INJECTION METHOD

A. Description of the Proposed Method

Assuming there are F_i ($i = 1, 2, \dots, 9$) faulty SMs that have been bypassed in-branch i , $v_{bi,0}$ and $v_{bi,com}$ need to be supported by $N - F_i$ SMs. Therefore, the per-unit (p.u.) value of $v_{bi,0}$ and $v_{bi,com}$, i.e., $v_{bi,0}^{pu}$ and $v_{bi,com}^{pu}$, can be expressed as (6), where U_C is the average capacitor voltage of each SM. It should be noted that the proposed method only uses the CMV to realize fault tolerance, and the U_C of the remaining healthy SMs will not increase after some SMs are failed, which is the premise of analysis and discussion in this article.

$$v_{bi,0}^{pu} = v_{bi,0}/(N - F_i)U_C, v_{bi,com}^{pu} = v_{bi,com}/(N - F_i)U_C. \quad (6)$$

Actually, $v_{bi,com}^{pu}$ is the reference modulation waveform of each healthy SM in branch i . To avoid overmodulation, $v_{bi,com}^{pu}$ should be limited in the range expressed as (7). D_{max} is the maximum duty ratio during the PWM process, which can be set to a reasonable value less than 1 according to the safe requirements of the system.

$$v_{bi,com}^{pu} \in [-D_{max}, D_{max}]. \quad (7)$$

When one of F_i is larger than a certain value, the maximum value of the corresponding $|v_{bi,0}^{pu}|$ may exceed D_{max} . Therefore, v_{com} needs to be injected in each branch to ensure that all $v_{bi,com}^{pu}$ are still in the range of (7). The maximum and minimum

available value of v_{com} , i.e., v_{com_max} and v_{com_min} , can be derived as (8), and v_{com} should be in the range of $[v_{com_min}, v_{com_max}]$. Obviously, $v_{com_max} \geq 0$ and $v_{com_min} \leq 0$ need to be guaranteed. When \hat{v}_{g1} and f_1 are fixed, v_{com_max} and v_{com_min} are functions of F_i , \hat{v}_{m2} , f_2 and θ , which do not have generalized analytical expressions.

$$v_{com_max} = \min \{ [D_{max}(N - F_i)U_C + v_{bi,0}] | i = 1, 2, \dots, 9 \}$$

$$v_{com_min} = \max \{ [-D_{max}(N - F_i)U_C + v_{bi,0}] | i = 1, 2, \dots, 9 \}. \quad (8)$$

Different from the NS method, the main idea of the proposed method is not to use a specific CMV form, but to calculate the optimum CMV in real-time according to the relationship between $v_{bi,0}^{pu}$ and D_{max} at any moment. Concretely, at any moment, if the maximum one of $v_{bi,0}^{pu}$ (denoted as $v_{bj,0}^{pu}$) is larger than D_{max} , the value of the excess part is taken as v_{com} , the same as the situation where the minimum one of $v_{bi,0}^{pu}$ (denoted as $v_{bk,0}^{pu}$) is less than $-D_{max}$. Finally, the CMV injected by the proposed method, i.e., v_{com_PM} , can be expressed as follows:

$$v_{com_PM} = (v_{bj,0}^{pu} - D_{max}) \times (N - F_j)U_C, \text{ if } v_{bj,0}^{pu} > D_{max}$$

$$v_{bj,0}^{pu} = \max \{ v_{bi,0}^{pu} | i = 1, 2, \dots, 9 \}, j \in \{1, 2, \dots, 9\}$$

$$v_{com_PM} = (v_{bk,0}^{pu} + D_{max}) \times (N - F_k)U_C, \text{ if } v_{bk,0}^{pu} < -D_{max}$$

$$v_{bk,0}^{pu} = \min \{ v_{bi,0}^{pu} | i = 1, 2, \dots, 9 \}, k \in \{1, 2, \dots, 9\}. \quad (9)$$

The p.u. value of v_{com_PM} in healthy SMs in branch i can be expressed as (10). $v_{com_PM,i}^{pu}$ may be different since F_i are not necessarily the same.

$$v_{com_PM,i}^{pu} = v_{com_PM} / (N - F_i)U_C. \quad (10)$$

In this way, $|v_{bj,com}^{pu}|$ or $|v_{bk,com}^{pu}|$ is always kept as D_{max} in the time range when $|v_{bj,0}^{pu}|$ or $|v_{bk,0}^{pu}|$ exceeds D_{max} . As long as v_{com_PM} is in the range of $[v_{com_min}, v_{com_max}]$, the other $|v_{bi,com}^{pu}|$ are all less than D_{max} after v_{com_PM} is injected, and v_{com_PM} calculated by (9) is a feasible solution which can ensure the normal operation of the M3C. Otherwise, it is impossible to avoid overmodulation for all branches by injecting CMV, which indicates that the numbers of faulty SMs exceed the safe values of the converter. Undoubtedly, there is no feasible solution for v_{com_PM} if the two cases in (9) occur simultaneously.

Fig. 2 presents the waveforms of $v_{bi,com}^{pu}$, $v_{bi,0}^{pu}$, and $v_{com_PM,4}^{pu}$ when $F_4/N, F_7/N$ are both 0.2679 and the others are all 0 under a specific load condition. It should be noted that to make the curves in Fig. 2 clearer, only several $v_{bi,com}^{pu}$ which should be focused on are presented. When $v_{b4,0}^{pu}$ is larger than D_{max} (i.e., 0.9 here), v_{com_PM} with a positive value is injected to limit $v_{b4,com}^{pu}$ to D_{max} . When v_{com_PM} reaches v_{com_max} which is determined by $v_{b8,0}$ at t_1 ($v_{b8,0}$ is the minimum one of $v_{bi,0}$ at t_1), $v_{b8,com}^{pu}$ reaches $-D_{max}$, which indicates that the available range of the CMV in (8) has been taken maximum utilization. Therefore, if F_4 further increases, v_{com_PM} calculated by (9) will exceed its available range and make $v_{b8,com}^{pu}$ less than $-D_{max}$, leading to overmodulation. This indicates that F_4/N has reached its maximum value in this situation, the same as F_7/N .

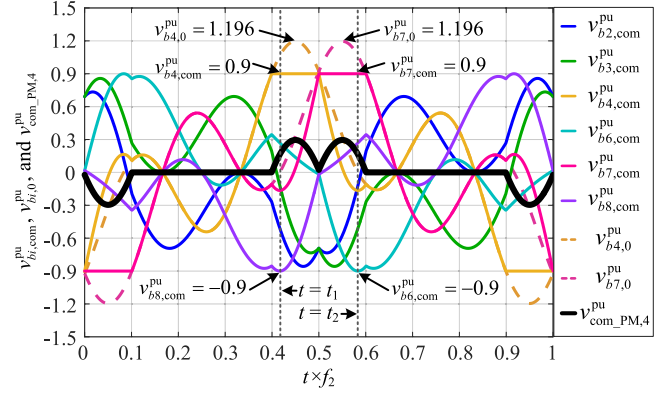


Fig. 2. Waveforms of $v_{bi,com}^{pu}$, $v_{bi,0}^{pu}$, and $v_{com_PM,4}^{pu}$ when using the proposed method under the condition that $m = 0.9$, $D_{max} = 0.9$, $\hat{v}_{m2} = \hat{v}_{g1}$, $f_2 = f_1/3$, and $\theta = 0$, where $F_4/N, F_7/N$ are both 0.2679 and the others are all 0.

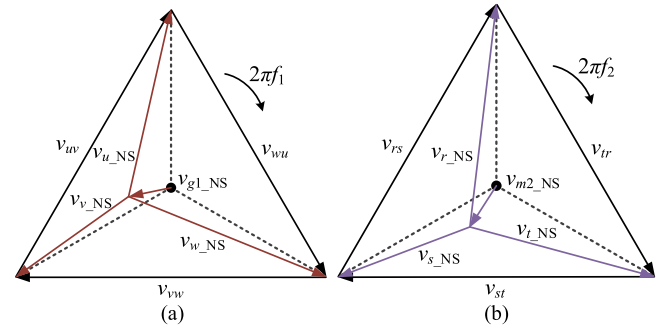


Fig. 3. Principle of the traditional NS method for the M3C. (a) Input side. (b) Output side.

It should be noted that m_{max} cannot be further increased by using the NS method. For instance, for the situation shown in Fig. 2, considering $v_{b4,com}^{pu}$ equals D_{max} and $v_{b8,com}^{pu}$ equals $-D_{max}$ at t_1 , the injection of any form of nonzero CMV will cause $v_{b4,com}^{pu}$ to be larger than D_{max} or $v_{b8,com}^{pu}$ to be less than $-D_{max}$ at t_1 , according to the expression of $v_{bi,com}$ in (5). This indicates that the available range of v_{com_PM} has been fully utilized by the proposed method, and m_{max} cannot be further increased by injecting any form of nonzero CMV.

B. Comparison Between the Existing NS Method

The basic principle of the existing NS method for the M3C is presented in Fig. 3. By adjusting the NS voltages of the input and output sides, i.e., v_{g1_NS} and v_{m2_NS} , the overmodulation of each branch is avoided without changing the line voltages of both sides. v_{g1_NS} and v_{m2_NS} are the equivalent CMVs injected by the NS method. The generalized form of the CMV injected by the NS method, i.e., v_{com_NS} , can be expressed as (11), which is composed of input and output orthogonal voltage components and determined by four coefficients, i.e., k_n ($n = 1, 2, 3, 4$).

$$v_{com_NS} = k_1 \hat{v}_{g1} \cos(\omega_1 t) + k_2 \hat{v}_{g1} \sin(\omega_1 t)$$

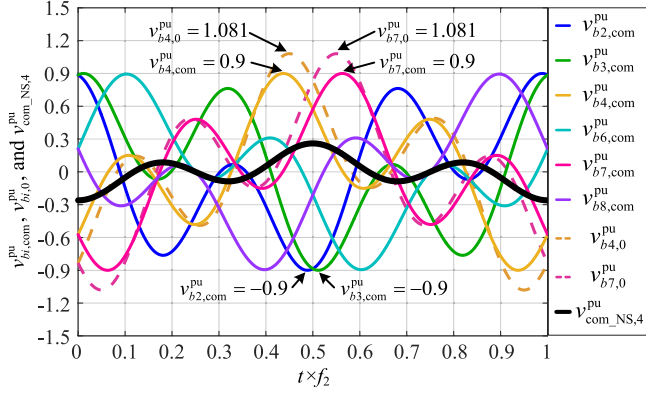


Fig. 4. Waveforms of $v_{bi,com}^{pu}$, $v_{bi,0}^{pu}$, and $v_{com_NS,4}^{pu}$ when using the traditional NS method under the condition that $m = 0.9$, $D_{max} = 0.9$, $\hat{v}_{m2} = \hat{v}_{g1}$, $f_2 = f_1 / 3$, and $\theta = 0$, where F_4 / N , F_7 / N are both 0.1898 and the others are all 0.

$$+ k_3 \hat{v}_{m2} \cos(\omega_2 t + \theta) + k_4 \hat{v}_{m2} \sin(\omega_2 t + \theta). \quad (11)$$

The optimum values of k_n which can maximize m_{max} can be defined as k_{n_NS} . Since the time-domain relationship between each $v_{bi,0}^{pu}$ change along with f_2 and θ , k_{n_NS} are related not only to the values of F_i but also to f_2 and θ . Therefore, k_{n_NS} can be expressed as a function of F_i , f_2 , and θ , i.e.,

$$k_{n_NS} = f(F_i, f_2, \theta), n = 1, 2, 3, 4. \quad (12)$$

Since the number of combinations of F_i , f_2 , and θ is infinite theoretically (considering that f_2 and θ are continuous variables), the calculated results will be very complex, and it is difficult to traverse all cases. Consequently, the optimized NS voltages are difficult to be stored as a lookup table for utilization. On the contrary, for the proposed adaptive optimum method, although there is no generalized analytical expression of v_{com_PM} , the injected v_{com_PM} is adaptive to various conditions with different F_i , f_2 / f_1 , and θ , since v_{com_PM} is calculated in real-time according to the relationship between $v_{bi,0}^{pu}$ and D_{max} . The proposed method is much more convenient for utilization.

To illustrate that the proposed method is better than the existing NS method in terms of maximizing m_{max} , the theoretical results of the proposed method and the NS method are compared under the same load condition. Fig. 4 presents the waveforms of $v_{bi,com}^{pu}$, $v_{bi,0}^{pu}$, and $v_{com_NS,4}^{pu}$ when the NS method is employed under the same load condition with Fig. 2. Different to Fig. 2, F_4 / N , F_7 / N are both 0.1898 in Fig. 4, which have been the maximum values when employing the NS method. As presented in Fig. 4, on the condition that $F_4 / N = F_7 / N = 0.1898$, the maximum values of $v_{b4,com}^{pu}$ and $v_{b7,com}^{pu}$ reach 0.9, and the minimum values of $v_{b2,com}^{pu}$, $v_{b3,com}^{pu}$, $v_{b6,com}^{pu}$, and $v_{b8,com}^{pu}$ are close to -0.9 . This indicates that k_n has reached their optimum value k_{n_NS} when using the NS method under this condition. The values of k_{n_NS} are $k_{1_NS} = -0.3145$, $k_{2_NS} = 0$, $k_{3_NS} = -0.2638$, and $k_{4_NS} = 0$. When F_4 or F_7 further increases, no matter how to adjust the value of k_n , the NS method cannot guarantee that all $|v_{bi,com}^{pu}|$ are limited within D_{max} . This implies that F_4 and F_7 have reached their maximum values when the

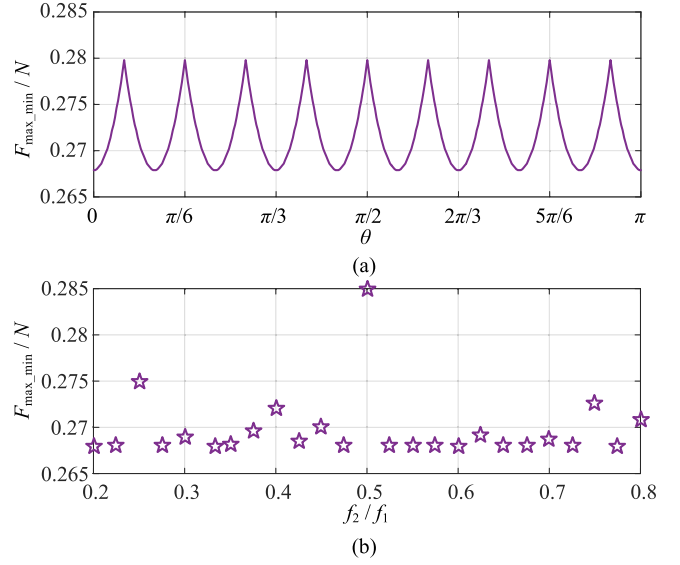


Fig. 5. Variation of F_{max_min} / N along with θ and f_2 / f_1 when $\hat{v}_{m2} = \hat{v}_{g1}$, and $m = m_{max} = D_{max}$. (a) $f_2 / f_1 = 1/3$ and θ changes. (b) $\theta = 0$ and f_2 / f_1 changes.

NS method is employed, which are 0.1898. However, F_4 / N is 0.2679 in Fig. 2. Therefore, when $m = D_{max} = 0.9$, the value of F_4 / N when using the proposed method can be increased by nearly 41% compared with that using the NS method. This also can be observed from the difference between the maximum value of $v_{b4,0}^{pu}$ in Figs. 2 and 4 [according to (6), the larger F_4 produces the larger $v_{b4,0}^{pu}$]. Consequently, the proposed method ensures that the M3C can support the rated maximum input and output voltage when more SMs fail. In other words, when F_i are identical, the value of m_{max} when employing the proposed method is larger than that when using the NS method, which is better than the NS method.

In fact, in terms of avoiding over-modulation of all branches, the absolute value of the CMV injected by the proposed method is minimal since it always limits the maximum one of $|v_{bi,com}^{pu}|$ to D_{max} . When m increases, both $|v_{com_min}|$ and $|v_{com_max}|$ will decrease. When the absolute value of the CMV reaches $|v_{com_min}|$ or $|v_{com_max}|$, m reaches m_{max} . Therefore, if the CMV with the minimum absolute value is always employed to avoid over-modulation within the range of $[v_{com_min}, v_{com_max}]$, it must be able to maximize m_{max} . Therefore, v_{com_PM} injected by the proposed method is the optimum one for maximizing m_{max} .

C. Discussion of the Operating Area

To study the operating area of the M3C after the fault, the maximum number of nonredundant faulty SMs in one branch is analyzed. Fig. 5 presents the analytical results under different θ and f_2 / f_1 . It should be noted that the condition that only one F_i (denoted as F_h) is not 0 but the other F_i ($i = 1, 2, \dots, 9$, $i \neq h$) are all 0 is considered here. In Fig. 5, F_{max_min} is the minimum one of the maximum values of F_i when the fault occurs in each branch in turn and m always maintains m_{max} .

In addition, the variation $\hat{v}_{m2}/\hat{v}_{g1}$ under the same m does not influence F_{\max_min}/N since it does not change the time-domain relationship between each $v_{bi,0}^{\text{pu}}$. It can be seen that F_{\max_min}/N varies in a certain range along with θ and f_2/f_1 , and its minimum value is 0.2679. Therefore, to ensure that the M3C can support the rated maximum input and output voltage under any θ and f_2/f_1 , F_i/N should not exceed 0.2679.

In addition, assuming that $m_{\max,1}$ is the value of m_{\max} on the condition that one of F_i , i.e., F_h , is M_1 ($0 \leq M_1 < N$) and the other F_i are all 0 while $m_{\max,2}$ is the value of m_{\max} when F_h is M_2 , the mathematical definition of $m_{\max,1}$ and $m_{\max,2}$ can be expressed as

$$\begin{aligned} m_{\max,1} &= m_{\max} \Big|_{F_h = M_1, h \in \{1, 2, \dots, 9\}, F_i = 0, i = 1, 2, \dots, 9, i \neq h} \\ m_{\max,2} &= m_{\max} \Big|_{F_h = M_2, h \in \{1, 2, \dots, 9\}, F_i = 0, i = 1, 2, \dots, 9, i \neq h} \end{aligned} \quad (13)$$

Then, the relationship between $m_{\max,1}$ and $m_{\max,2}$ can be derived as follows:

$$m_{\max,1}/m_{\max,2} = (2 - M_1/N)/(2 - M_2/N). \quad (14)$$

By setting $m_{\max,1} = D_{\max}$ and $M_1/N = 0.2679$, the values of m_{\max} under different F_h/N (i.e., $m_{\max,2}$ under different M_2/N) can be calculated according to (14), which can be utilized to determine the operating area of the M3C with different numbers of no redundant faulty SMs.

The cases in which other F_i are also not zero in addition to F_h can be divided into two categories.

The first case is that all branches with F_i not 0 are in the same row or column in the M3C topology. For example, F_1, F_4 , and F_7 are not 0, whereas other F_i are 0. In this case, the largest one of F_1, F_4 , and F_7 can be regarded as M_2 in (14) to calculate $m_{\max,2}$. For instance, when $F_4 \geq F_1 \geq F_7$, the value of F_4 can be directly substituted to calculate $m_{\max,2}$. Although F_1 and F_7 are not 0 at this time, their values do not have effect on m_{\max} of the M3C. The reason is that the three branches in the same row or column always contain the input or output fundamental voltage component with a phase difference of $2\pi/3$. Regardless of how f_2 and θ change, the fundamental voltages of any two of the three branches in the same row or column will not be the maximum and minimum one of all branches at the same time. According to (8), the available CMV range of the M3C is determined by the fundamental voltages of the two branches with the largest and smallest amplitude at the same moment. Therefore, when F_i are not 0 in the three branches in the same row or column, the fundamental voltages of the two branches with smaller F_i do not effect on the CMV range, which does not affect m of the M3C.

The second case is that all branches with F_i not 0 are not in the same row or column in the M3C topology. For example, $F_4 \geq F_7 \geq F_8 > 0$, while other F_i are 0. As shown in Fig. 2, at the moment t_1 , $v_{b4,\text{com}}^{\text{pu}}$ reaches 0.9 and $v_{b8,\text{com}}^{\text{pu}}$ reaches -0.9 when $F_4/N = 0.2679$ and $F_8/N = 0$. If F_8 is not 0, $v_{b8,\text{com}}^{\text{pu}}$ will be less than -0.9 at the moment t_1 and cause overmodulation, which means that the value of m when F_8/N is not 0 under the condition of Fig. 2 should be reduced. In this case, the expression

TABLE I
EXPERIMENTAL PARAMETERS

Parameters	Value	Parameters	Value
SMs per branch	$N = 3$	Grid voltage	$\hat{v}_{g1} = 130$ V
Carrier frequency	$f_s = 2$ kHz	Output voltage	$\hat{v}_{m2} = 130$ V
Rated capacitor voltage	$U_c^* = 100$ V	R - L load	$R_L = 15$ Ω $L_L = 10$ mH

of (14) should be changed to (15)

$$m_{\max,1}/m_{\max,2} = (2 - M_1/N)/(1 + F_{\text{sec}}/N - M_2/N). \quad (15)$$

In (15), F_{sec} is the largest F_i of the branches which are not in the same row or column as branch h (assuming $m_{\max,1} = D_{\max}$ and $M_1/N = 0.2679$ in (15), and F_h is the variable which is set to M_2 to calculate $m_{\max,2}$). It should be noted that F_{sec} should be less than F_h , or the roles of F_{sec} and F_h should be interchanged. For instance, when $F_4 \geq F_7 \geq F_8$, F_{sec} is F_8 , and F_h is F_4 . In contrast, when $F_8 \geq F_7 \geq F_4$, F_{sec} is F_7 , and F_h is F_8 . As a result, $m_{\max,2}$ in the second case can be calculated.

IV. EXPERIMENTAL RESULTS

An M3C prototype with three SMs in each branch (27 SMs in total) is built to verify the proposed method. The method proposed in [12] is utilized to realize the branch energy balancing control (BEBC). Four digital-to-analog converters are employed to present the waveforms of $v_{bi,\text{com}}^{\text{pu}}$ and $v_{\text{com_PM},i}^{\text{pu}}$. Experimental parameters are shown in Table I, and an R - L load is employed. In addition, f_1 is 50 Hz, f_2 is 50/3 Hz, and θ is 0. The whole experimental condition is similar to the theoretical analysis condition of Fig. 2.

Fig. 6 presents the experimental results of the proposed method. In Fig. 6, v_{rs} , v_{st} , and v_{tr} are output line voltages, and $u_{c(i,1)}$ is the capacitor voltage of the first SM in branch i . $v_{b4,\text{com}}^{\text{pu}*}$ is the per-unit value of reference branch voltage with circulating voltage excluded (“*” means the reference value, the same as the others). Before the moment t_1 , there is no faulty SM in the prototype and it operates normally. At t_1 , assuming that SM_(4,1) (the first SM in branch 4) is failed and bypassed (the time required for fault detection is neglected to verify the steady-state performance), the available voltage of branch 4 is not enough to support $v_v - v_r$ all the time. As a result, CMV is injected to ensure that $v_{b4,\text{com}}^{\text{pu}*}$ is limited within $\pm D_{\max}$, which is set to 0.9 in the experiment. When $v_{b4,\text{com}}^{\text{pu}*}$ reaches 0.9, $v_{b8,\text{com}}^{\text{pu}*}$ is close to -0.9 . This indicates that m reaches its maximum value under this condition, which equals 0.866 according to the parameters in Table I. On the other hand, assuming $m_{\max,1} = D_{\max} = 0.9$ and $M_1/N = 0.2679$ in (14), while M_2/N is the value corresponding to the experiment condition, i.e., 1/3, it can be calculated that the theoretical value of $m_{\max,2}$ is also 0.866, which is in accord with the experimental parameters and results. This proves the validity of (14). Then, at t_2 , SM_(7,1) is also failed and bypassed. The injected CMV is adjusted automatically according to the

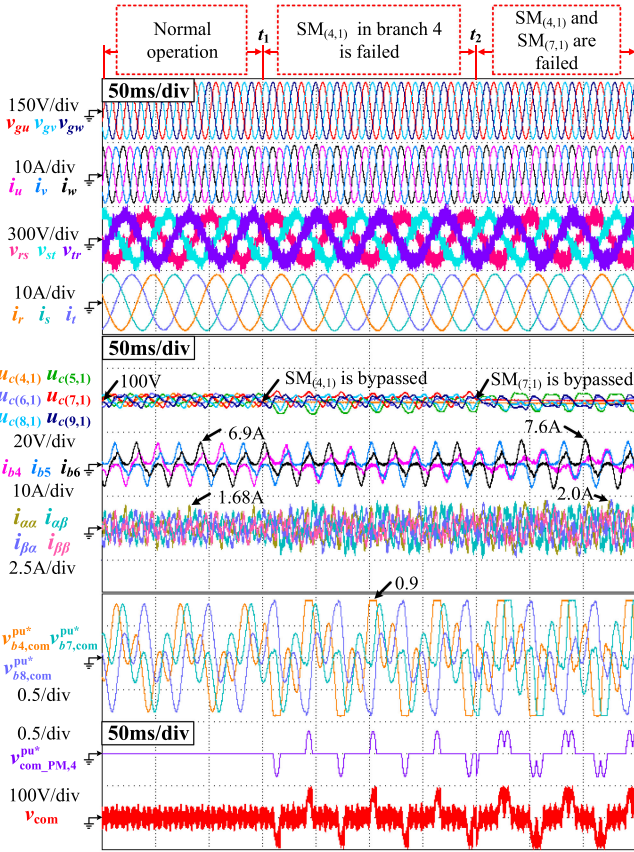


Fig. 6. Experimental results of the proposed method when $SM_{(4,1)}$ and $SM_{(7,1)}$ are failed and bypassed one by another.

rule expressed by (9), and $v_{b4,com}^{pu*}$ and $v_{b7,com}^{pu*}$ are both limited within ± 0.9 . Meanwhile, it can be seen that the waveform of $v_{com_PM,4}^{pu*}$ is consistent with that in Fig. 2. In the whole process, the injection of the CMV can ensure the stable operation of the M3C and has no significant impact on the input and output currents in the steady state, which remain symmetrical after the fault.

In addition, the injected CMV of the proposed method contains a certain amount of the input and output fundamental components, which will lead to the variation of the branch dc power distribution and affect the branch energy balance. Thus, the BEBC will produce circulating currents with fundamental components to ensure capacitor voltage balance after a dynamic process. As a result, the maximum amplitude of the circulating currents increases from 1.68 (under the normal condition) to 2A (when $SM_{(4,1)}$ and $SM_{(7,1)}$ are failed), which increases by about 20% after the SM fault. Meanwhile, the circulating currents produced by the BEBC lead to variations in branch currents after the SM fault. The maximum amplitude of the branch currents increases from 6.9 to 7.6A, which increases by about 10% after the fault. However, considering that this increment is the result when 33% of nonredundant SMs in branches 4 and 7 are failed, the increment of the current stress caused by the proposed method is not significant.

To compare the input and output currents before and after the fault in the frequency domain, Figs. 7 and 8 show the

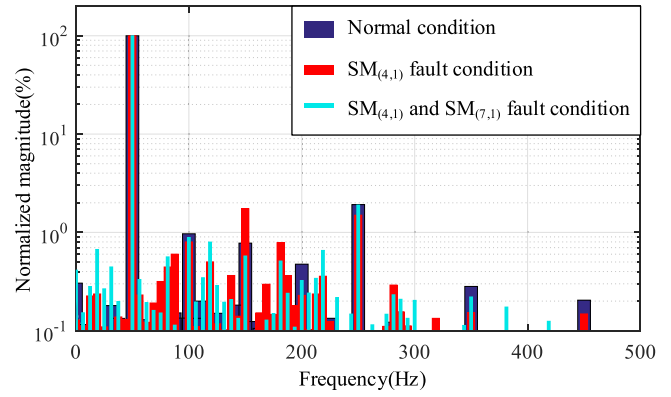


Fig. 7. Frequency spectrum of i_u under normal and SM fault conditions.

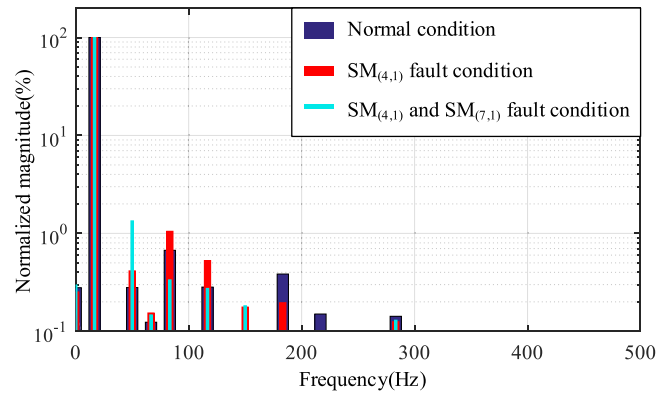


Fig. 8. Frequency spectrum of i_r under normal and SM fault conditions.

TABLE II
THDS OF THE INPUT AND OUTPUT CURRENTS UNDER DIFFERENT CONDITIONS

Operating conditions	THD_{i_g}	THD_{i_m}
Normal	2.77%	1.18%
$SM_{(4,1)}$ is failed	3.11%	1.57%
$SM_{(4,1)}$ and $SM_{(7,1)}$ are failed	2.96%	1.71%

spectrum of i_u and i_r under normal and SM fault conditions, respectively. Regardless of whether the nonredundant SM fault occurs in one branch (i.e., $SM_{(4,1)}$ is failed) or two branch (i.e., $SM_{(4,1)}$ and $SM_{(7,1)}$ are failed), only the amplitudes of several harmonic components increase in the frequency spectrums of i_u and i_r . However, the overall increments are not significant, and the frequency spectrums of input and output currents do not deteriorate obviously. The total harmonic distortions (THDs) of input and output currents under different conditions are further calculated, with the results shown in Table II. In Table II, THD_{i_g} and THD_{i_m} represent the THD of input and output currents respectively, which are the average values of three-phase currents. It can be seen that THD_{i_g} and THD_{i_m} after the SM fault increase no more than 0.55% compared to those under normal conditions. Thus, the THDs of the input and output currents are not significantly affected when employing the proposed method. In conclusion, although the CMV injected by the proposed

method will maintain the branch voltage at a fixed value for a period of time, it does not have significant impacts on the frequency spectrums and THDs of input and output currents after the SM fault.

V. CONCLUSION

This letter proposes an adaptive optimum CMV injection method to realize the fault tolerance of the M3C under the fault of nonredundant SMs. When the fundamental reference voltage of a certain branch exceeds the limitation of its available voltage, the excess part is taken as the CMV to be injected in each branch. The calculated CMV is automatically adjusted in real-time, which is adaptive to various load and fault conditions. Therefore, the proposed method is much easier to be employed than the existing NS methods. What is more, since the proposed method always employs the CMV with the minimal amplitude to avoid overmodulation of each branch, the injected CMV can maximize the IOVR, which is also the optimum one. The operating area of the M3C when the fault of nonredundant SMs occurs in one branch is also analyzed. The results suggest that the M3C can still support the rated maximum input and output voltage when the number of nonredundant faulty SMs in one branch is less than 26.79% of the total nonredundant SMs. Experimental results have verified the effectiveness of the proposed method and the analysis of the operating area, which also proves that the proposed method does not have obvious influence on the THD of the input and output currents after the fault.

REFERENCES

- [1] M. Diaz, E. Ibaceta, A. Duran, C. Melendez, M. Urrutia, and F. Rojas, "Field oriented control of a modular multilevel matrix converter based variable speed drive," in *Proc. 21st Eur. Conf. Power Electron. Appl.*, Genova, Italy, 2019, pp. P.1–P.6.
- [2] S. Liu, X. Wang, Y. Meng, P. Sun, H. Luo, and B. Wang, "A decoupled control strategy of modular multilevel matrix converter for fractional frequency transmission system," *IEEE Trans. Power Del.*, vol. 32, no. 4, pp. 2111–2121, Aug. 2017.
- [3] J. Kucka, D. Karwatzki, and A. Mertens, "AC/AC modular multilevel converters in wind energy applications: Design considerations," in *Proc. 18th Eur. Conf. Power Electron. Appl.*, Karlsruhe, Germany, 2016, pp. 1–10.
- [4] M. Diaz, R. Cardenas, E. Ibaceta, A. Mora, and P. Wheeler, "An overview of applications of the modular multilevel matrix converter," *Energies*, vol. 13, no. 21, pp. 5546–5582, Oct. 2020.
- [5] M. Vasiladiotis, R. Baumann, C. Häderli, and J. Steinke, "IGCT-based direct AC/AC modular multilevel converters for pumped hydro storage plants," in *Proc. IEEE Energy Convers. Congr. Expo.*, Portland, OR, USA, 2018, pp. 4837–4844.
- [6] Q. Yang, J. Qin, and M. Saedifard, "A postfault strategy to control the modular multilevel converter under submodule failure," *IEEE Trans. Power Del.*, vol. 31, no. 6, pp. 2453–2463, Dec. 2016.
- [7] J. Kucka, D. Karwatzki, and A. Mertens, "Enhancing the reliability of modular multilevel converters using neutral shift," *IEEE Trans. Power Electron.*, vol. 32, no. 12, pp. 8953–8957, Dec. 2017.
- [8] S. Farzamkia, H. Iman-Eini, M. Noushak, and A. Hadizadeh, "Improved fault-tolerant method for modular multilevel converters by combined DC and neutral-shift strategy," *IEEE Trans. Ind. Electron.*, vol. 66, no. 3, pp. 2454–2462, Mar. 2019.
- [9] S. Farzamkia, M. Noushak, H. Iman-Eini, A. Khoshkbar-Sadigh, and S. Farhangi, "Fault-tolerant method to reduce voltage stress of submodules in postfault condition for regenerative MMC-based drive," *IEEE Trans. Ind. Electron.*, vol. 68, no. 6, pp. 4718–4726, Jun. 2021.
- [10] S. Farzamkia, H. Iman-Eini, A. Khoshkbar-Sadigh, and M. Noushak, "A software-based fault-tolerant strategy for modular multilevel converter using DC bus voltage control," *IEEE J. Emerg. Sel. Topics Power Electron.*, vol. 9, no. 3, pp. 3436–3445, Jun. 2021.
- [11] J. Kucka, D. Karwatzki, and A. Mertens, "Optimised operating range of modular multilevel converters for AC/AC conversion with failed modules," in *Proc. 17th Eur. Conf. Power Electron. Appl.*, Geneva, Switzerland, 2015, pp. 1–10.
- [12] W. Kawamura, M. Hagiwara, and H. Akagi, "Control and experiment of a modular multilevel cascade converter based on triple-star bridge cells," *IEEE Trans. Ind. Appl.*, vol. 50, no. 5, pp. 3536–3548, Sep./Oct. 2014.